APPLIED SCIENCES AND ENGINEERING

# Metadisorder for designer light in random systems

**Sunkyu Yu, Xianji Piao, Jiho Hong, Namkyoo Park***

2016 © The Authors, some rights reserved; exclusive licensee American Association for the Advancement of Science. Distributed under a Creative Commons Attribution NonCommercial License 4.0 (CC BY-NC).

**Disorder plays a critical role in signal transport by controlling the correlation of a system, as demonstrated in various complex networks. In wave physics, disordered potentials suppress wave transport, because of their localized eigenstates, from the interference between multiple scattering paths. Although the variation of localization with tunable disorder has been intensively studied as a bridge between ordered and disordered media, the general trend of disorder-enhanced localization has remained unchanged, and the existence of complete delocalization in highly disordered potentials has not been explored. We propose the concept of "metadisorder": randomly coupled optical systems in which eigenstates can be engineered to achieve unusual localization. We demonstrate that one of the eigenstates in a randomly coupled system can always be arbitrarily molded, regardless of the degree of disorder, by adjusting the self-energy of each element. Ordered waves with the desired form are then achieved in randomly coupled systems, including plane waves and globally collective resonances. We also devise counterintuitive functionalities in disordered systems, such as "small-world–like" transport from non–Anderson-type localization, phase-conserving disorder, and phase-controlled beam steering.**

## INTRODUCTION

Network modeling has provided an intuitive picture to understand various complex systems in nature and society. In these system networks, disorder is a crucial factor in signal transport over the system. For example, in the pioneering work in graph theory (*1*), D. J. Watts discovered "small-world disordered networks" with randomly rewired connections, which can model various elemental systems in physics, biology, and sociology: seismic networks (*2*), *Caenorhabditis elegans* neurons (*3*), brain connectome (*4*), and affinity groups in social networks (*1*).

The role of disorder is also evident in wave physics, especially when compared to the "order" in potential energy, such as periodic or quasi-periodic potentials. Periodic potentials allow ballistic transport through extended Bloch eigenstates (*5*), whereas broken correlation in disordered potentials leads to Anderson-localized eigenstates (*6*–*8*), which significantly suppress wave transport. Although serious attempts have been made (*8*–*12*) to fill the gap between the order and disorder in wave systems, the increase of disorder has only led to a monotonic change from extended to localized eigenstates (*9*), prohibiting the existence of eigenstates with unusual forms: for example, completely delocalized eigenstates in highly disordered potentials. Thus, a clear distinction has been maintained between the applications of order and disorder in wave systems, in accordance with the contrast between their eigenstates: transporting devices using ordered potentials (*5*, *13*) and focusing devices using disordered potentials (*14*–*16*). In disordered systems, the design of nontrivial waves such as globally collective and scattering-free propagations remains a challenge.

Here, we demonstrate the existence of globally collective and delocalized waves in randomly coupled optical systems, by introducing the concept of "metadisorder." By using platforms of coupled waveguides (or resonators), we prove that designer mode excitation and wave propagation can be achieved in the random network by controlling the self-energy of the optical elements (for example, size and loss and gain of waveguides) (Fig. 1). Distinct from random scattering and Anderson localization in classical random systems (Fig. 1, A and B), unusual phenomena are demonstrated in the "artificial" disordered optical potentials (Fig. 1, C and D): perfect plane waves without any scattering or phase distortion, designer guided waves, globally collective resonances, conservative waves in complex potentials, and the invisible disorder of phase conservation, all of which provide ordered waves with disorder-like energy bands. By creating artificial disorder to achieve non–Anderson-type localization, we also reveal the separate control of eigenstate localization and wave transport, analogous to the separation of transport and clustering in the "small-world network" (*1*). Our method, paving the way toward disorder-robust small-world optics, is also applied to functional wave devices in randomly coupled optical systems, including tunable focusing, in-phase spatial oscillation, parity converters, point-source excitation of plane waves, and modal filtering from incoherent light sources.

Photonic Systems Laboratory, Department of Electrical and Computer Engineering, Seoul National University, Seoul 08826, Korea.
*Corresponding author. Email: nkpark@snu.ac.kr

## RESULTS

### Wave transport and localization in randomly coupled systems

We start with random systems composed of weakly coupled optical elements, such as waveguides (*5*, *17*) or resonators (*18*, *19*). On the basis of discrete models of coupled-mode theory (CMT) (*17*, *20*) or tight-binding (TB) analysis (*19*), an $N$-body system is governed by the eigenvalue equation $H\psi = \gamma\psi$ (see Materials and Methods). The Hamiltonian $H$ can be decomposed into $H = D + K$, where $D$ is the diagonal matrix for the self-energy of each optical element [for example, wavevector $\beta$ of each waveguide or resonant frequency $f$ of each resonator, both of which define the phase evolution of the field in uncoupled optical elements (*20*)], and $K$ is the off-diagonal matrix for the interaction energy between elements [for example, coupling coefficient $\kappa$ between coupled waveguides or between coupled resonators (*20*)], which represents the network of the system. Figure 2A shows a one-dimensional (1D) randomly coupled system with off-diagonal disorder (*21*), having the identical self-energy $\beta$ and disordered interactions $\{[D]_p = \gamma_{o0}$ and $[K]_{pq} = \kappa_{pq} = \kappa_0 + \Delta\kappa \cdot u(-1,1)$, where $\kappa_{pq}$ is the coupling between the $p$th and $q$th elements for $1 \le p, q \le N$, $\kappa_0$ and $\Delta\kappa$ represent the averaged and disordered coupling, respectively, and $u$ is the uniform probability density function$\}$.

Figure 2 (B to D) presents a few eigenstates of the optical systems at different degrees of off-diagonal disorder (*21*) (see note S1 for its practical realization in the mid-infrared regime). As the strength of the disorder $\Delta\kappa$ increases, Bloch eigenstates (Fig. 2B) begin to be localized (Fig. 2C), eventually exhibiting the wavelength-scale Anderson localization

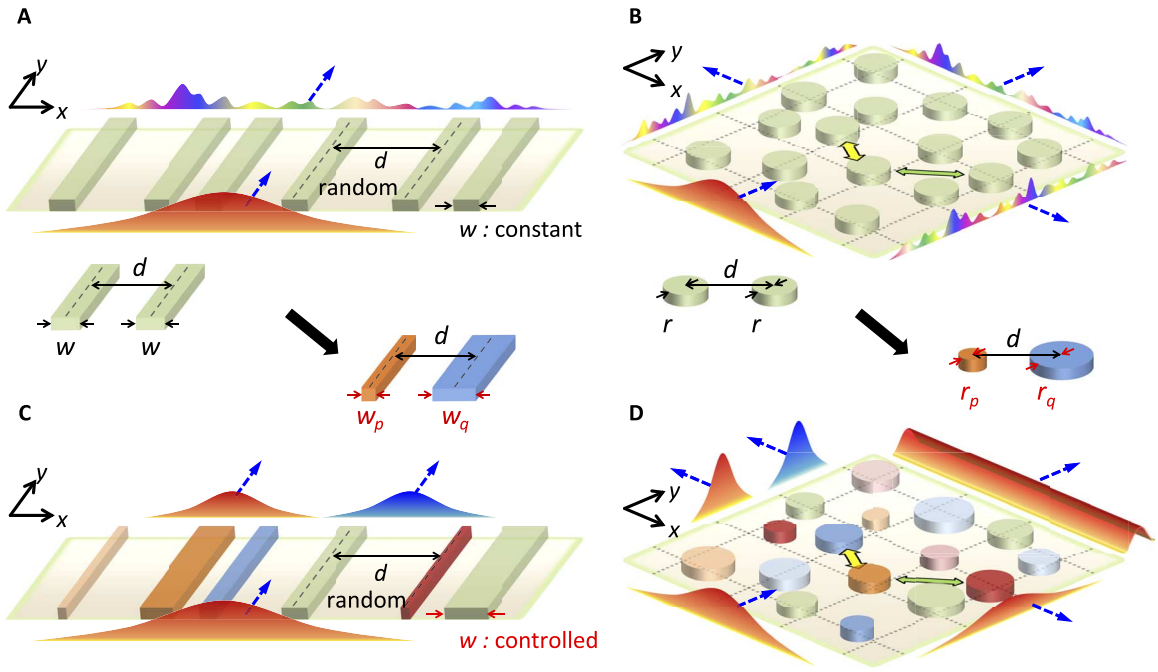


**Fig. 1. The concept of metadisorder systems.** (**A** and **B**) Random scattering and Anderson localization in randomly coupled systems composed of identical waveguides (constant widths *w*) (A) or resonators (constant radii *r*) (B). (**C** and **D**) Delocalized propagations of designer modal profiles in metadisorder systems. The control of self-energy distributions can be obtained by manipulating the waveguide widths $w_{p,q}$ (C) or the resonator radii $r_{p,q}$ (D). The positions of optical elements in coupled systems are assumed to be completely random. Blue dotted arrows denote propagation directions.

of exponential decay envelopes (Fig. 2D). The localization naturally results in the suppression of wave transport within the network, from ballistic (Fig. 2E; $\alpha = 2$) to diffusive (Fig. 2F; $1 < \alpha < 2$) and even subdiffusive (Fig. 2G; $\alpha < 1$) transport [$\alpha$, diffusion exponent (*22*); see Materials and Methods]. Not restricted to eigenstate localization (Fig. 2H; *w*, modal width; see Materials and Methods and note S2) and the following forms of suppressed wave transport (Fig. 2I), the increase of the disorder in the system also alters the spreading of its eigenvalues, linearizing the eigenband (Fig. 2J and note S3). In these results, a continuous transition between the regimes of order and disorder is evident, confirming the classical relationship (*6*–*12*) between localization, transport, and disorder. Motivated by the generic form of the Hamiltonian $H = D + K$, we now demonstrate that the design of unconventional eigenstates in highly disordered potentials can be achieved by using the degree of freedom on the self-energy of each element in *D*, which was neglected in Fig. 2.

## Molding of an eigenstate in randomly coupled systems

Suppose that we desire to "mold" an eigenstate $\psi$ with the spatial distribution of $v_m = [v_{m1}, v_{m2},\ldots, v_{mN}]^T$ with the eigenvalue $\gamma_m$ while preserving the randomly coupled network of the system. We design such a system in the reciprocal space basis; one of its basis vectors has the spatial distribution of $v_m$. For this purpose, we develop the eigen-decomposition matrix $V = [v_m, v_2,\ldots, v_N]$ using the Gram-Schmidt process, where $v_m$ and the set of column vectors $v_s = [v_{s1}, v_{s2},\ldots, v_{sN}]^T$ ($s = 2, 3,\ldots, N$) together compose the orthonormal basis set. Because of the orthonormality ($VV^\dagger = I$), the eigenvalue equation in the *V*-reciprocal space becomes $V^\dagger HV(V^\dagger\psi) = \gamma(V^\dagger\psi)$, or $H_r\psi_r = \gamma\psi_r$, where $H_r = V^\dagger HV$ and $\psi_r = V^\dagger\psi$. The randomly coupled network of the system is represented by a complex matrix $K_r = V^\dagger KV$ in the *V*-reciprocal space, and then, the *V*-reciprocal Hamiltonian $H_r = V^\dagger DV + K_r$ has the following components

$$H_r = \begin{bmatrix} \sum_p v^*_{mp}\gamma_{op}v_{mp} + K_{r11} & \sum_p v^*_{mp}\gamma_{op}v_{2p} + K_{r12} & \cdots & \sum_p v^*_{mp}\gamma_{op}v_{Np} + K_{r1N} \\ \sum_p v^*_{2p}\gamma_{op}v_{mp} + K_{r21} & \sum_p v^*_{2p}\gamma_{op}v_{2p} + K_{r22} & \cdots & \sum_p v^*_{2p}\gamma_{op}v_{Np} + K_{r2N} \\ \vdots & \vdots & \ddots & \vdots \\ \sum_p v^*_{Np}\gamma_{op}v_{mp} + K_{rN1} & \sum_p v^*_{Np}\gamma_{op}v_{2p} + K_{rN2} & \cdots & \sum_p v^*_{Np}\gamma_{op}v_{Np} + K_{rNN} \end{bmatrix} \quad (1)$$

where $\gamma_{op} = [D]_p$ and $K_{rpq} = [K_r]_{pq}$. To design the eigenstate $\psi$ of spatial representation $v_m$, one of the reciprocal eigenstates should be $\psi_r = [1, 0, \ldots, 0]^T$. This condition is uniquely fulfilled when the first column of $H_r$ has only one nonzero component of $[H_r]_{11}$, and its eigenvalue can always be set as desired by assigning $[H_r]_{11} = \gamma_m$. We then achieve the self-energy of each element $\gamma_{op}$ deterministically as follows (see Materials and Methods), from $[[H_r]_{11}, [H_r]_{21},\ldots, [H_r]_{N1}]^T = [\gamma_m, 0,\ldots, 0]^T$

$$\begin{bmatrix} \gamma_{o1} \\ \gamma_{o2} \\ \vdots \\ \gamma_{oN} \end{bmatrix} = \left( \begin{bmatrix} v^*_{m1} & v^*_{m2} & \cdots & v^*_{mN} \\ v^*_{21} & v^*_{22} & \cdots & v^*_{2N} \\ \vdots & \vdots & \ddots & \vdots \\ v^*_{N1} & v^*_{N2} & \cdots & v^*_{NN} \end{bmatrix} \begin{bmatrix} v_{m1} & 0 & \cdots & 0 \\ 0 & v_{m2} & \cdots & 0 \\ \vdots & \vdots & \ddots & \vdots \\ 0 & 0 & \cdots & v_{mN} \end{bmatrix} \right)^{-1} \begin{bmatrix} \gamma_m - K_{r11} \\ -K_{r21} \\ \vdots \\ -K_{rN1} \end{bmatrix} \quad (2)$$

or, simply, $\gamma_o = [\gamma_{o1}, \gamma_{o2},\ldots, \gamma_{oN}]^T = [\mathrm{diag}(v_m)]^{-1}V[\gamma_m - K_{r11}, -K_{r21},\ldots, -K_{rN1}]^T$.

Equation 2 indicates that if the inverse of the matrix $diag(v_m)$ exists, that is, $v_{mi} \neq 0$ for all *i*, the self-energy vector $\gamma_o$ can always be

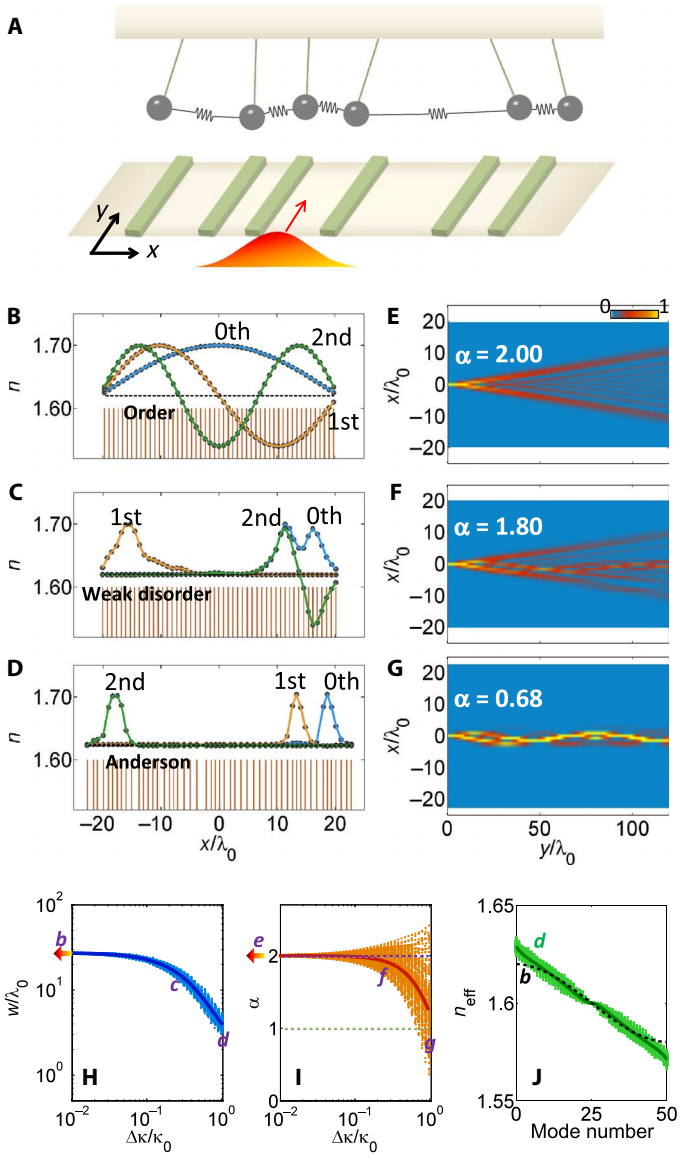


**Fig. 2. Effect of disorder in optical systems.** (**A**) A schematic of a random optical system composed of coupled waveguides, analogous to the randomly coupled pendulums with identical oscillating features. The oscillation of each pendulum describes the phase evolution during propagation. (**B** to **D**) The first three eigenstates for ordered (B), weakly disordered (C), and Anderson (D) potentials, calculated by using CMT (see Materials and Methods). The potential *n* denotes the effective waveguide index of a single waveguide. (**E** to **G**) Corresponding wave transport calculated by using the transfer-matrix method (TMM) (see Materials and Methods). (**H** and **I**) The variations of modal size *w* (H) and diffusion exponent α (I) are shown as a function of the disorder Δκ. (**J**) Eigenbands ($n_{eff}$) for the disorder in (B) (black dotted line) and (D) (green points and line). The points in (H) to (J) represent each statistical ensemble, and the solid lines are the averages of 200 ensembles. The green dotted line in (I) denotes the diffusion state (α = 1). $\gamma_{o0} = 1.6 \cdot k_0$, $\kappa_0 = 0.01 \cdot k_0$, and $N = 51$ for (B) to (J), where $k_0 = 2\pi/\lambda_0$ is the free-space wave number. The practical waveguide design and the distance between waveguides in the mid-infrared regime ($\lambda_0 = 3$ μm) are calculated in note S1 using COMSOL Multiphysics.

found, determining the optical potential of each element from $\gamma_{op}$ (see fig. S1C for $\gamma_o = n$). Therefore, for *any* network *K* regardless of the degree of disorder, a single eigenstate can always be molded into the desired shape of $v_m$ with the eigenvalue $\gamma_m$ by adjusting the potential of each element (Fig. 2A versus Fig. 3A) while preserving the network of the system, which we herein call metadisorder to describe the artificial change (engineered *D*) of the disordered system (random *K*). The proposed metadisorder system allows for the nontrivial form of an eigenstate in all regimes of disordered networks *K*, for example, the globally collective eigenstate, in contrast to the case of identical elements (Fig. 2, C and D). We note that such a degree of freedom for an eigenstate in an *N*-body system originates from the *N* number of the adjustable design parameters, the self-energy of *N* elements, in an $N \times N$ Hamiltonian matrix.

## 1D metadisorder systems for designer waves and non-Anderson localization

Figure 3 shows examples of designer waves in 1D metadisorder systems, where the optical potential of each waveguide is calculated using Eq. 2. Compared to the highly disordered system composed of identical waveguides in Fig. 2, we achieve various examples of wave systems having a designer eigenstate $v_m$: plane wave (Fig. 3B), Gaussian-enveloped guided wave with nonexponential decay (Fig. 3C), and interface (Fig. 3D) and surface (Fig. 3E) waves both with Anderson-like (*6*, *9*, *10*, *21*) exponential decay. We note that the real-valued $v_m$ corresponds to the designer ground state in the disordered eigenband (red arrows in Fig. 3, F to I; see note S4 for designer excited states, which allow conservative waves in complex potentials).

Our design method allows for a scattering-free plane wave in highly disordered systems (Fig. 3B; $\Delta\kappa = \kappa_0$), in stark contrast to conventional disordered systems (Fig. 2G), which only lead to strong localization from random scattering. The plane wave eigenstate in highly disordered systems, which has a modal size equal to the overall system size, is more extended than that in finite-*N* ordered systems with the field discontinuity at the boundary due to the broken translational symmetry (Fig. 2B; see also note S5 for the stability of the delocalization in metadisorder systems, against self-energy and coupling errors). Furthermore, unconventional localization forms, such as the non-Anderson Gaussian localization (Fig. 3C) or the designed Anderson-like exponential localization at the interface (Fig. 3D) or surface (Fig. 3E), can also be achieved as a general extension to the accidental emergence of classical Anderson localization (Fig. 2D). Because a potential with a globally extended eigenstate should have the reduced random scattering in the overall system, other eigenstates of similar eigenvalues also tend to have wider spatial bandwidth. We note that the designed eigenstates in metadisorder systems can be excited through the evanescent coupling (*23*) from a single waveguide (note S6).

The concept of metadisorder also creates a new class of disordered potentials, which support the counterintuitive relation between eigenstate localization (*w*) and transport (α) by imposing the designer eigenstate $v_m$ with unconventional localizations. In Fig. 4, we consider the localized designer eigenstate of the specific form $v_m(x) = \exp[-|x|^g/(2 \cdot \sigma^g)]$ (Fig. 4A), where $g = 1$ for Anderson-like exponential localization and $g = 2$, 4, and 6 for the convenient examples of non-Anderson localizations. Figure 4 (F to N) presents the localization-transport (*w*-α) relation of 1D non-Anderson metadisorder systems compared to classical Anderson disorder (Fig. 4B) and Anderson-like metadisorder (Fig. 4, C to E). Although Anderson-like metadisorders ($g = 1$) provide a similar *w*-α relation to that of Anderson disorder (Fig. 4B versus Fig. 4, C to E), the non-Anderson metadisorder ($g > 1$) enables more "localized" waves yet achieves ballistic transport (for example, Fig. 4B versus Fig. 4F; a factor of ~2 decrease for *w*, and $\alpha \approx 2$, for $\Delta\kappa < \kappa_0/10$), analogous to the separate control of localization and transport in "small-world" networks (*1*). Such a nonclassical wave transport even enables "disorder-induced"

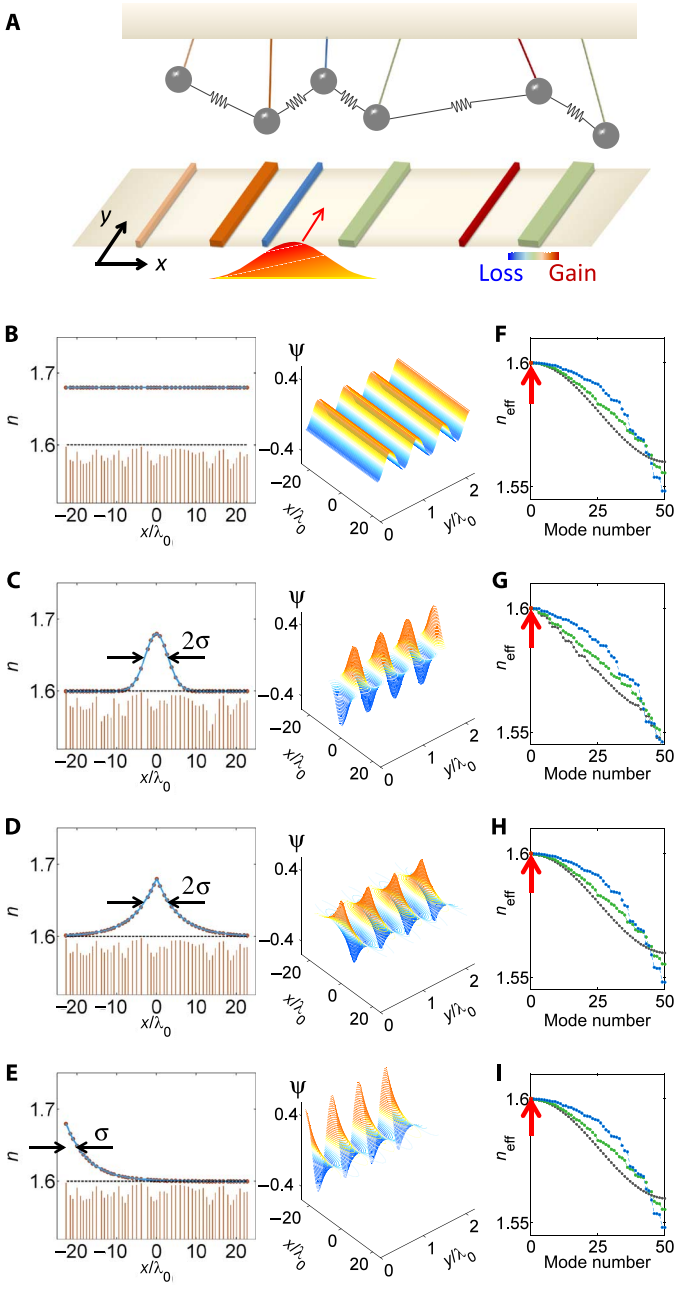


**Fig. 3. 1D metadisorder systems.** (**A**) A schematic of a 1D metadisorder system composed of coupled waveguides, analogous to the randomly coupled pendulums with different self-oscillating features, such as oscillating period (rod length) and gain or loss parameters (color). Each waveguide has different real parts of self-energy due to changing the width of the waveguide (note S1). The colors of the waveguides represent the imaginary part of self-energy: gain and loss (treated in note S4). (**B** to **I**) Designed eigenstates and optical potentials, eigenstate propagations (B to E), and eigenvalues ($n_{eff}$) (F to I) of 1D metadisorder systems are calculated by using the CMT for plane wave ($v_m(x) = 1$) (B and F), Gaussian wave ($v_m(x) = \exp[-x^2/(2\cdot\sigma^2)]$) (C and G), interface wave ($v_m(x) = \exp[-|x|/(2\cdot\sigma)]$) (D and H), and surface wave ($v_m(x) = \exp[-|x-x_L|/(2\cdot\sigma)]$) (E and I) eigenstates, where the spatial bandwidth $\sigma = L_{st}/16$ in (C) to (E) and (G) to (I), the left boundary $x_L = -L_{st}/2$, and $L_{st}$ is the overall potential length. $\Delta\kappa = \kappa_0$ in (B) to (E) for the extreme degree of disorder. Blue symbols represent $\Delta\kappa = \kappa_0$, green symbols represent $\Delta\kappa = 0.53\cdot\kappa_0$, and black dotted lines represent $\Delta\kappa = 0$ in (F) to (I). All of the other parameters are the same as those in Fig. 2, based on note S1.

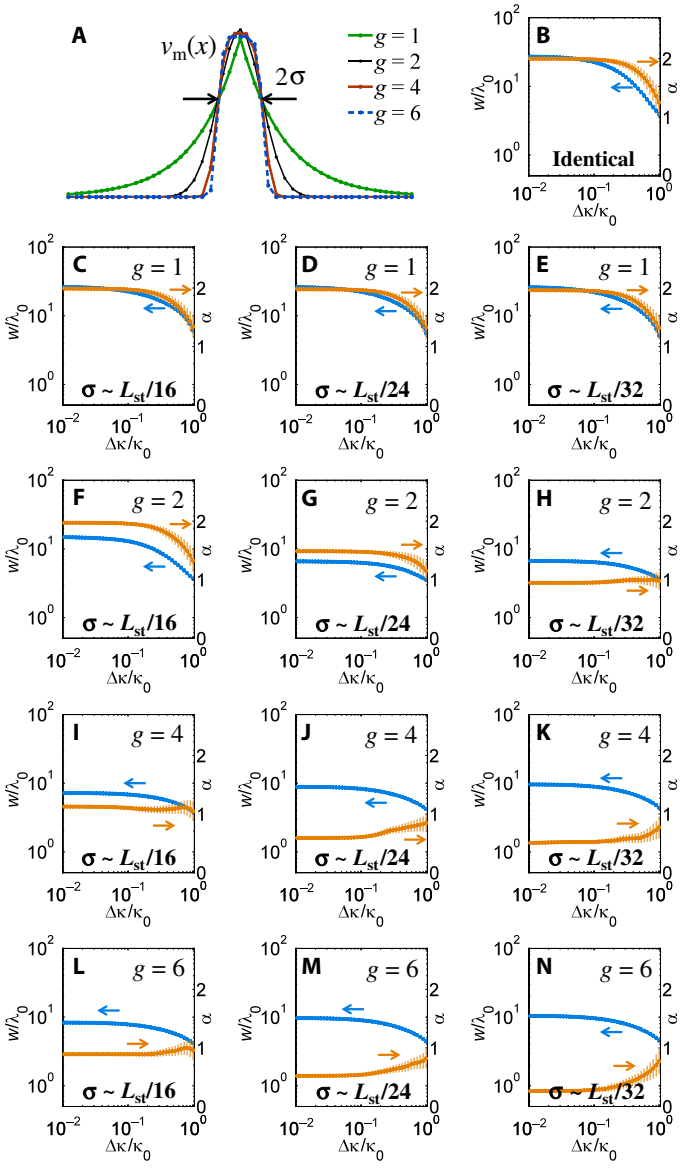


**Fig. 4. Non-Anderson metadisorder systems with disorder-induced wave transport.** (**A**) Shapes of designer eigenstates $v_m(x) = \exp[-|x|^g/(2\cdot\sigma^g)]$ with different $g$. (**B** to **N**) Eigenstate localization ($w$) and wave transport ($\alpha$) for Anderson disorder with identical elements (B), g = 1 Anderson-like metadisorders (C to E), and $g = 2$ (F to H), $g = 4$ (I to K), and $g = 6$ (L to N) non-Anderson metadisorders . In metadisorder systems, the bandwidths of designer eigenstates are $\sigma = L_{st}/16$ (C, F, I, and L), $\sigma = L_{st}/24$ (D, G, J, and M), and $\sigma = L_{st}/32$ in (E, H, K, and N). Error bars denote the SD of 200 ensembles in (B) to (N). All of the other parameters are the same as those in Fig. 2, based on note S1.

wave transport [increase in α for smaller values of $w(\Delta\kappa)$ or σ; Fig. 4H], showing the reversed relation between $w$ and α compared to that of conventional disordered systems (*7*–*10*, *17*). This anomalous relation is more apparent for metadisorder systems with larger $g$ (Fig. 4, I to N; for $g = 4$ and 6), allowing not only separate control of localization and wave transport with $g$ and σ but also robustness of wave transport to the disorder Δκ, analogous to the difference between clustering and characteristic path length in small-world networks (*1*).

### Extension to 2D metadisorder systems for designer wave functionalities

The eigenstate design in a *V*-reciprocal space allows for its extension to multidimensional problems in a straightforward manner by including all of the coupling coefficients in a multidimension in the network matrix *K*. Here, we consider 2D disordered systems, obtained by the random deformation of the periodic lattice (Fig. 5A). Figure 5B shows an example of disordered coupled resonator systems from the random deformation of a 17 × 17 square lattice (see note S7 for the practical realization of 2D coupled resonator systems in the terahertz regime).

Figure 5 (C to H) and movies S1 to S6 show collective and ordered light behaviors in highly disordered systems, which support strongly correlated phase information over the entire system. By adjusting each resonant frequency of constituent resonators following Eq. 2, we design

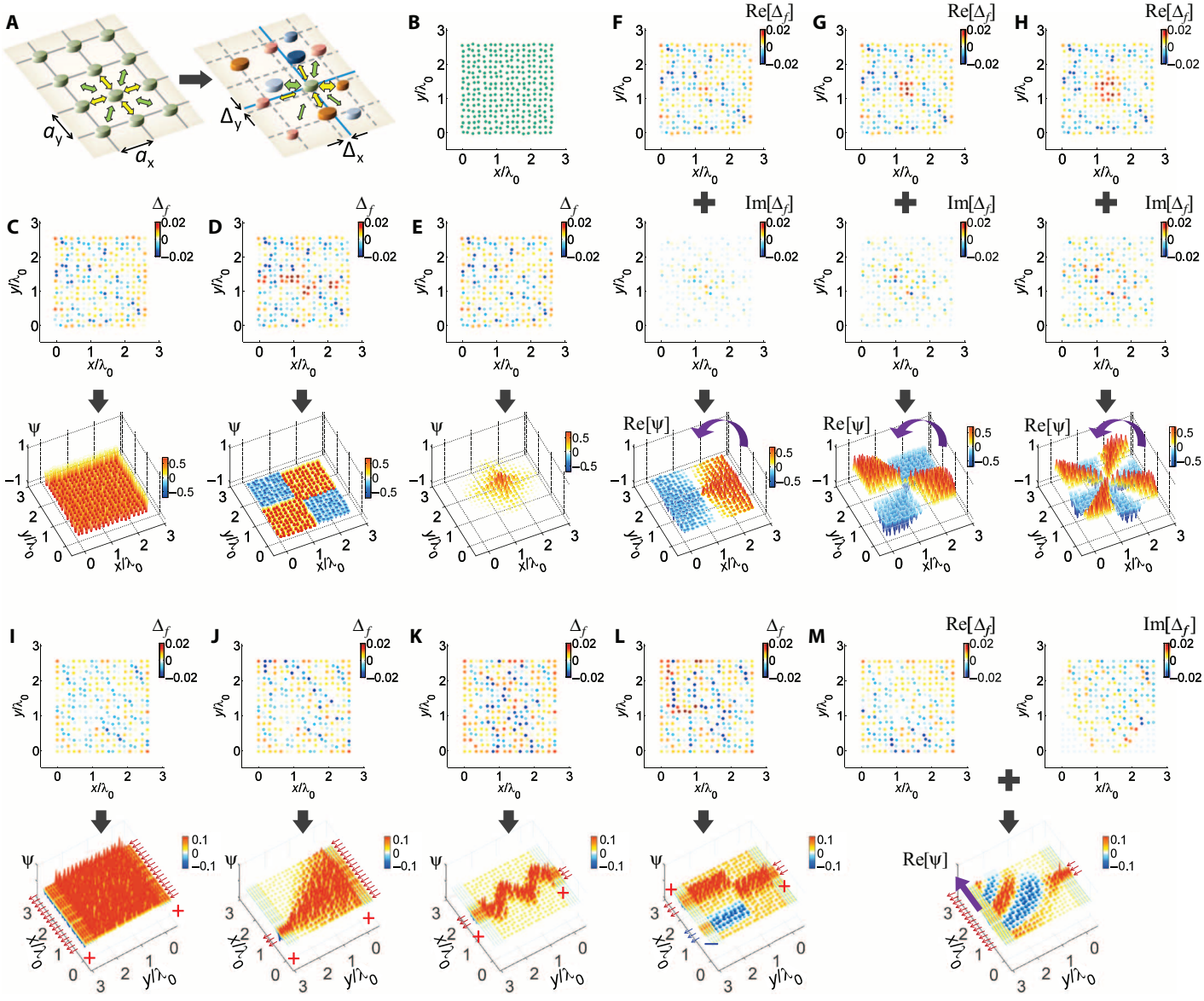


**Fig. 5. 2D metadisorder systems.** (**A**) Schematics of a coupled resonator lattice with identical elements (left) and its metadisorder-transformed structure (right). The self-energy of each element in the metadisorder system is adjusted by controlling the size of the resonator or using gain or loss materials. Nearest-neighbor (yellow arrows) and next-nearest-neighbor (green arrows) couplings are presented. (**B** to **M**) 2D metadisorder systems. The practical weak-coupling design for the CMT analysis is calculated in note S7, using COMSOL Multiphysics, for the terahertz regime ($\lambda_0 = c/f_0 = 265.3$ μm). For the periodicity of $a_x = a_y = 0.16 \cdot \lambda_0$, the position of each resonator is randomly shifted by $\Delta_x = \Delta_y = 0.03 \cdot \lambda_0 \cdot u(-1, 1)$ in (B) to (M), and the self-energy of each element is adjusted by $f_0 \cdot (1 + \Delta_f)$ following the metadisorder design from Eq. 2. (B) A sample of the obtained resonator distribution for the 17 × 17 lattice in (C) to (H). (C to E) Standing-wave collective resonances using real potentials for uniform (C), quadrupole (D), and exponentially localized (E) distributions. (F to H) Traveling-wave chiral collective resonances, using complex potentials, for dipole (F), quadrupole (G), and octopole (H) distributions. (I to M) Metadisorder-based functionalities in the 17 × 17 lattice for invisible disorder (I), steered focusing (J), spatial oscillation (K), parity-converted beam splitter (L), and the point-source excitation of oblique plane waves (M). The fields in input and output waveguides (I to M) are multiplied by 40 for better visualization. The designed resonance is set to $\gamma_m = f_0$ for all cases. See movies S1 to S11 for the temporal dynamics of each case in (C) to (M).

free-form standing-wave resonances with a perfectly uniform field distribution (Fig. 5C), quadrupole phase distribution (Fig. 5D), and designed localization (Fig. 5E), despite randomly deformed interactions between resonators. Furthermore, the introduction of complex potentials allows for one-way traveling-wave resonances, for example, by imposing the form of $\exp(-i\rho\theta)$ on $\nu_m$ (Fig. 5, F to H, for the azimuth $\theta$). Such a "chiral" rotation of the phase in collective resonances derives the orbital angular momentum (OAM) (*24*) of resonant light. Notably, although the chiral feature of light in the proposed metadisorder systems also requires complex optical potentials with gain and loss, our method involves neither parity-time symmetry nor periodicity (*25*). Propagating light with nonzero OAM can also be achieved by using waveguide-based disordered systems.

Finally, having demonstrated collective resonance modes in highly disordered systems, we present the excitation of designer eigenstates (Fig. 5, I to M, and movies S7 to S11) with the external coupling of conventional waveforms. When the inner connection of the system is sufficiently strong, the separation of eigenvalues (that is, free spectral range) becomes sufficiently large to achieve wave dynamics dependent solely on a single eigenstate. Figure 5I and movie S7 show the wave flow through the perfectly uniform collective eigenstate over the entire system. Following the property of the eigenstate, the disordered system becomes "invisible" for incident plane waves, prohibiting any alteration of phase and amplitude [transmission (*T*), ~100%; zero effective index]. With eigenstate-based metadisorder design, we also implement high-level functionalities with excellent throughputs, including tunable light focusing (Fig. 5J; *T*, ~96%), phase-conserved spatial oscillation (Fig. 5K; *T*, ~98%), parity converters (even to odd) (Fig. 5L; *T*, ~99%) of real potentials, and the point-source excitation of oblique plane waves (5.6°) (Fig. 5M and movie S11; *T*, ~97%) using complex potentials. Because of the spectral selectivity of the designed eigenstate, metadisorder systems also allow the modal filtering function, or the excitation of target waveforms from spatially incoherent incidences (note S8).

## DISCUSSION

To summarize, we revealed a new class of random wave systems, that is, the metadisorder, which can be globally collective and deliberately controlled. Exploiting metadisorders of non–Anderson-type localization, we first derive the counterintuitive relation between localization and transport, including small-world–like (*1*) or disorder-induced transport. As demonstrated in collective wave dynamics and functionalities, our eigenstate-based approach also provides a powerful means to control wave flow while preserving or manipulating the phase information. Although we controlled only the self-energy $D$ for the Hamiltonian $H = D + K$, our method can also be easily extended to determine the "network" $K$ of disordered self-energy distributions for the designer eigenstate, revealing the unexplored regime between order and disorder from the correlation between diagonal (or self-energy) and off-diagonal (or interaction energy) disorders. We emphasize that our method is distinct from other approaches to handling the flow of waves: the supersymmetric technique (*23*, *26*–*28*) controls eigenspectra but transforms eigenstates in a fixed manner, and the transformation optics technique (*29*) treats a "continuous" potential landscape, lacking the degree of freedom in interaction energy. From their small-world–inherited disorder robustness and globally collective features, we also envisage the application of metadisorder systems to many other nontrivial physics, such as hyperuniformity (*30*, *31*), topological networks (*18*), or quasiparticles in disordered potentials.

## MATERIALS AND METHODS

### Analysis of randomly coupled discrete optical systems

Consider the $N$-body system composed of weakly coupled optical elements. In CMT (*17*) or TB (*19*) methods, the governing equation, including self-energy and interaction energy, becomes

$$\frac{d}{d\xi}\psi_p = i\gamma_{op}\psi_p + \sum_{q\neq p} i\kappa_{pq}\psi_q \tag{3}$$

where $p = (1, 2,\ldots, N)$ is the element number, $\psi_p$ is the field at the $p$th element, $\xi$ is the wave evolution axis [time $t$ for coupled resonators (*13*) and space $x$, $y$, or $z$ for coupled waveguides (*17*)], $\gamma_{op}$ is the self-energy of the $p$th element, and $\kappa_{pq}$ is the coupling coefficient between the $p$th and $q$th elements. For the steady-state solution ($\partial_\xi \rightarrow i\gamma$), Eq. 3 becomes the matrix eigenvalue problem $H\psi = \gamma\psi$, where

$$H = \begin{bmatrix} \gamma_{o1} & \kappa_{12} & \cdots & \kappa_{1N} \\ \kappa_{21} & \gamma_{o2} & \cdots & \kappa_{2N} \\ \vdots & \vdots & \ddots & \vdots \\ \kappa_{N1} & \kappa_{N2} & \cdots & \gamma_{oN} \end{bmatrix}$$

$$= D + K = \begin{bmatrix} \gamma_{o1} & 0 & \cdots & 0 \\ 0 & \gamma_{o2} & \cdots & 0 \\ \vdots & \vdots & \ddots & \vdots \\ 0 & 0 & \cdots & \gamma_{oN} \end{bmatrix} + \begin{bmatrix} 0 & \kappa_{12} & \cdots & \kappa_{1N} \\ \kappa_{21} & 0 & \cdots & \kappa_{2N} \\ \vdots & \vdots & \ddots & \vdots \\ \kappa_{N1} & \kappa_{N2} & \cdots & 0 \end{bmatrix} \tag{4}$$

$\psi = [\psi_1, \psi_2,\ldots, \psi_N]^T$, $D$ is the diagonal self-energy matrix, and $K$ is the off-diagonal network matrix. The randomly coupled system can then be described by assigning random numbers to the components of the $K$ matrix. Because each element number $p$ corresponds to the physical location of the $p$th element $\mathbf{X}_p$ [for example, $p \rightarrow x_p$ for 1D and $p \rightarrow (x_p, y_p)$ for 2D problems], the obtained eigenstate $\psi$ can be reexpressed in the spatial domain $\psi = \psi(\mathbf{X})$.

### Calculation of the diffusion exponent α

Consider the 1D system of Fig. 2 ($\xi = y$), which has an eigenstate of $\psi_k(x)$ and corresponding eigenvalues $\gamma_k$ ($k = 1, 2,\ldots, N$; $\gamma_k$ is the effective wavevector of $\psi_k$). For the incidence of $\varphi_i(x) = \Sigma a_k\cdot\psi_k$, the propagating field can be obtained through the TMM as $\varphi(x,y) = \Sigma a_k\cdot\psi_k\cdot\exp(i\gamma_k\cdot y)$. To analyze the transporting feature of the system without boundary effects, the incident wave was excited at the center waveguide [$x = x_m$, where $m = (N + 1)/2$ for odd $N$]; we then calculated the spatially varying mean-square displacement (MSD) (*22*) $M(y)$ as follows

$$M(y) = \langle x^2 \rangle = \frac{\sum_p (x_p - x_m)^2 \cdot |\phi(x_p, y)|^2}{\sum_p |\phi(x_p, y)|^2} \tag{5}$$

When the MSD $M(y)$ was fitted for $y$ exponentially as $M(y) \approx c_\alpha\cdot y^\alpha$, we achieved the diffusion exponent α: α = 2 for ballistic transport and α = 1 for diffusive transport (*22*). The calculated results are shown in Figs. 2 (E to G and I) and 4. Note that $m$ does not have to be the center waveguide precisely when $N$ is sufficiently large, and thus, the boundary effect can be neglected.

### Calculation of modal size

For the 1D system ($\xi = y$) with $\psi_k(x)$ and $\gamma_k$, the modal size for each eigenstate is defined as (*9*)

$$w_k = \frac{\left[\sum_{p=1}^{N} \left|\psi_k(x_p)\right|^2 \bullet \Delta x_p\right]^2}{\sum_{p=1}^{N} \left|\psi_k(x_p)\right|^4 \bullet \Delta x_p} \tag{6}$$

where $\Delta x_p$ is the size of the $p$th element, obtained from the distance between waveguides for each value of the coupling coefficient (see note S1). See also note S2 for the eigenstate-dependent localizations.

### The derivation of Eq. 2

The relation $[[H_r]_{11}, [H_r]_{21}, \ldots, [H_r]_{N1}]^T = [\gamma_m, 0, \ldots, 0]^T$ in the main text, for the design of $\psi$ of spatial representation $v_m$, has the following explicit form

$$\begin{bmatrix} \sum_p v_{mp}^* \gamma_{op} v_{mp} + K_{r11} \\ \sum_p v_{2p}^* \gamma_{op} v_{mp} + K_{r21} \\ \vdots \\ \sum_p v_{Np}^* \gamma_{op} v_{mp} + K_{rN1} \end{bmatrix} = \begin{bmatrix} \gamma_m \\ 0 \\ \vdots \\ 0 \end{bmatrix} \tag{7}$$

Equation 7 can be recast into the form of

$$\begin{bmatrix} v_{m1}^* & v_{m2}^* & \cdots & v_{mN}^* \\ v_{21}^* & v_{22}^* & \cdots & v_{2N}^* \\ \vdots & \vdots & \ddots & \vdots \\ v_{N1}^* & v_{N2}^* & \cdots & v_{NN}^* \end{bmatrix} \begin{bmatrix} v_{m1} & 0 & \cdots & 0 \\ 0 & v_{m2} & \cdots & 0 \\ \vdots & \vdots & \ddots & \vdots \\ 0 & 0 & \cdots & v_{mN} \end{bmatrix} \begin{bmatrix} \gamma_{o1} \\ \gamma_{o2} \\ \vdots \\ \gamma_{oN} \end{bmatrix}$$

$$= \begin{bmatrix} \gamma_m - K_{r11} \\ -K_{r21} \\ \vdots \\ -K_{rN1} \end{bmatrix} \tag{8}$$

Solving Eq. 8 for $\gamma_o = [\gamma_{o1}, \gamma_{o2}, \ldots, \gamma_{oN}]^T$, we arrived at Eq. 2 in the main text, with the condition of $v_{mi} \neq 0$ for all $i$.

## SUPPLEMENTARY MATERIALS

Supplementary material for this article is available at http://advances.sciencemag.org/cgi/content/full/2/10/e1501851/DC1

note S1. Design of waveguide-based 1D random networks.
note S2. Eigenstate-dependent localization.
note S3. The variation of the eigenband by disorders.
note S4. Designer excited states in 1D metadisorder systems.
note S5. Stability of the delocalization in metadisorder systems.
note S6. The excitation of the designer eigenstate in metadisorder systems.
note S7. Design of resonator-based 2D random optical networks.
note S8. Modal filtering through 2D metadisorder structures.
fig. S1. The design of waveguide-based elements for 1D random networks.
fig. S2. The localization of each eigenstate.
fig. S3. The variation of the eigenband for different degrees of disorder $\Delta\kappa$.
fig. S4. 1D metadisorder systems with complex potentials.
fig. S5. The variation of the ground-state modal size.
fig. S6. The excitation of designer eigenstates through the evanescent coupling.
fig. S7. The design of resonator-based elements for 2D random networks.
fig. S8. Modal filtering through 2D metadisorder systems, from incoherent source.
movie S1. Temporal wave dynamics of Fig. 5C.
movie S2. Temporal wave dynamics of Fig. 5D.
movie S3. Temporal wave dynamics of Fig. 5E.
movie S4. Temporal wave dynamics of Fig. 5F.
movie S5. Temporal wave dynamics of Fig. 5G.
movie S6. Temporal wave dynamics of Fig. 5H.
movie S7. Temporal wave dynamics of Fig. 5I.
movie S8. Temporal wave dynamics of Fig. 5J.
movie S9. Temporal wave dynamics of Fig. 5K.
movie S10. Temporal wave dynamics of Fig. 5L.
movie S11. Temporal wave dynamics of Fig. 5M.
References (*32*–*46*)

## REFERENCES AND NOTES


1. D. J. Watts, S. H. Strogatz, Collective dynamics of 'small-world'networks. *Nature* **393**, 440–442 (1998).
2. S. Abe, N. Suzuki, Small-world structure of earthquake network. *Physica A* **337**, 357–362 (2004).
3. S. Li, C. M. Armstrong, N. Bertin, H. Ge, S. Milstein, M. Boxem, P.-O. Vidalain, J.-D. J. Han, A. Chesneau, T. Hao, D. S. Goldberg, N. Li, M. Martinez, J.-F. Rual, P. Lamesch, L. Xu, M. Tewari, S. L. Wong, L. V. Zhang, G. F. Berriz, L. Jacotot, P. Vaglio, J. Reboul, T. Hirozane-Kishikawa, Q. Li, H. W. Gabel, A. Elewa, B. Baumgartner, D. J. Rose, H. Yu, S. Bosak, R. Sequerra, A. Fraser, S. E. Mango, W. M. Saxton, S. Strome, S. van den Heuvel, F. Piano, J. Vandenhaute, C. Sardet, M. Gerstein, L. Doucette-Stamm, K. C. Gunsalus, J. W. Harper, M. E. Cusick, F. P. Roth, D. E. Hill, M. Vidal, A map of the interactome network of the metazoan *C. elegans*. *Science* **303**, 540–543 (2004).
4. E. T. Bullmore, D. S. Bassett, Brain graphs: Graphical models of the human brain connectome. *Annu. Rev. Clin. Psychol.* **7**, 113–140 (2011).
5. D. N. Christodoulides, F. Lederer, Y. Silberberg, Discretizing light behaviour in linear and nonlinear waveguide lattices. *Nature* **424**, 817–823 (2003).
6. P. W. Anderson, Absence of diffusion in certain random lattices. *Phys. Rev.* **109**, 1492 (1958).
7. D. S. Wiersma, Disordered photonics. *Nat. Photonics.* **7**, 188–196 (2013).
8. D. S. Wiersma, P. Bartolini, A. Lagendijk, R. Righini, Localization of light in a disordered medium. *Nature* **390**, 671–673 (1997).
9. T. Schwartz, G. Bartal, S. Fishman, M. Segev, Transport and Anderson localization in disordered two-dimensional photonic lattices. *Nature* **446**, 52–55 (2007).
10. Y. Lahini, A. Avidan, F. Pozzi, M. Sorel, R. Morandotti, D. N. Christodoulides, Y. Silberberg, Anderson localization and nonlinearity in one-dimensional disordered photonic lattices. *Phys. Rev. Lett.* **100**, 013906 (2008).
11. N. Papasimakis, V. A. Fedotov, Y. H. Fu, D. P. Tsai, N. I. Zheludev, Coherent and incoherent metamaterials and order-disorder transitions. *Phys. Rev. B* **80**, 041102 (2009).
12. A. N. Poddubny, M. V. Rybin, M. F. Limonov, Y. S. Kivshar, Fano interference governs wave transport in disordered systems. *Nat. Commun.* **3**, 914 (2012).
13. J. D. Joannopoulos, S. G. Johnson, J. N. Winn, R. D. Meade, *Photonic crystals: molding the flow of light* (Princeton Univ. Press, Princeton, 2008).
14. M. Leonetti, S. Karbasi, A. Mafi, C. Conti, Light focusing in the Anderson regime. *Nat. Commun.* **5**, 4534 (2014).
15. A. P. Mosk, A. Lagendijk, G. Lerosey, M. Fink, Controlling waves in space and time for imaging and focusing in complex media. *Nat. Photonics* **6**, 283–292 (2012).
16. J.-H. Park, C. Park, H. Yu, J. Park, S. Han, J. Shin, S. H. Ko, K. T. Nam, Y.-H. Cho, Y. Park, Subwavelength light focusing using random nanoparticles. *Nat. Photonics* **7**, 454–458 (2013).
17. I. L. Garanovich, S. Longhi, A. A. Sukhorukov, Y. S. Kivshar, Light propagation and localization in modulated photonic lattices and waveguides. *Phys. Rep.* **518**, 1–79 (2012).
18. G. Q. Liang, Y. D. Chong, Optical resonator analog of a two-dimensional topological insulator. *Phys. Rev. Lett.* **110**, 203904 (2013).
19. E. Lidorikis, M. M. Sigalas, E. N. Economou, C. M. Soukoulis, Tight-binding parametrization for photonic band gap materials. *Phys. Rev. Lett.* **81**, 1405 (1998).
20. H. A. Haus, *Waves and Fields in Optoelectronics* (Prentice-Hall, New Jersey, 1984).
21. L. Martin, G. Di Giuseppe, A. Perez-Leija, R. Keil, F. Dreisow, M. Heinrich, S. Nolte, A. Szameit, A. F. Abouraddy, D. N. Christodoulides, B. E. A. Saleh, Anderson localization in optical waveguide arrays with off-diagonal coupling disorder. *Opt. Express* **19**, 13636–13646 (2011).
22. K. Hahn, J. Kärger, V. Kukla, Single-file diffusion observation. *Phys. Rev. Lett.* **76**, 2762 (1996).
23. M.-A. Miri, M. Heinrich, R. El-Ganainy, D. N. Christodoulides, Supersymmetric optical structures. *Phys. Rev. Lett.* **110**, 233902 (2013).

24. G. Molina-Terriza, J. P. Torres, L. Torner, Twisted photons. *Nat. Phys.* **3**, 305–310 (2007).
25. S. Yu, H. S. Park, X. Piao, B. Min, N. Park, Low-dimensional optical chirality in complex potentials. *Optica* **3**, 1025–1032 (2016).
26. S. Yu, X. Piao, J. Hong, N. Park, Bloch-like waves in random-walk potentials based on supersymmetry. *Nat. Commun.* **6**, 8269 (2015).
27. S. Longhi, Supersymmetric transparent optical intersections. *Opt. Lett.* **40**, 463–466 (2015).
28. M.-A. Miri, M. Heinrich, D. N. Christodoulides, Supersymmetry-generated complex optical potentials with real spectra. *Phys. Rev. A* **87**, 043819 (2013).
29. J. B. Pendry, D. Schurig, D. R. Smith, Controlling electromagnetic fields. *Science* **312**, 1780–1782 (2006).
30. S. Torquato, F. H. Stillinger, Local density fluctuations, hyperuniformity, and order metrics. *Phys. Rev. E* **68**, 041113 (2003).
31. S. Torquato, G. Zhang, F. Stillinger, Ensemble theory for stealthy hyperuniform disordered ground states. *Phys. Rev. X* **5**, 021020 (2015).
32. J. Kischkat, S. Peters, B. Gruska, M. Semtsiv, M. Chashnikova, M. Klinkmüller, O. Fedosenko, S. Machulik, A. Aleksandrova, G. Monastyrskyi, Mid-infrared optical properties of thin films of aluminum oxide, titanium dioxide, silicon dioxide, aluminum nitride, and silicon nitride. *Appl. Opt.* **51**, 6789–6798 (2012).
33. K. Okamoto, *Fundamentals of optical waveguides* (Academic Press, Cambridge, 2010).
34. A. Szameit, F. Dreisow, T. Pertsch, S. Nolte, A. Tünnermann, Control of directional evanescent coupling in fs laser written waveguides. *Opt. Express* **15**, 1579–1587 (2007).
35. F. A. B. F. de Moura, M. L. Lyra, Delocalization in the 1D Anderson model with long-range correlated disorder. *Phys. Rev. Lett.* **81**, 3735 (1998).
36. G. Theodorou, M. H. Cohen, Extended states in a one-demensional system with off-diagonal disorder. *Phys. Rev. B* **13**, 4597 (1976).
37. T. Saitoh, T. Mukai, 1.5 μm GaInAsP traveling-wave semiconductor laser amplifier. *IEEE J. Quant. Electron.* **23**, 1010–1020 (1987).
38. R. I. Laming, M. N. Zervas, D. N. Payne, Erbium-doped fiber amplifier with 54 dB gain and 3.1 dB noise figures. *IEEE Photon. Technol. Lett.* **4**, 1345–1347 (1992).
39. Z. Bakonyi, H. Su, G. Onishchukov, L. F. Lester, A. L. Gray, T. C. Newell, A. Tunnermann, High-gain quantum-dot semiconductor optical amplifier for 1300 nm. *IEEE J. Quantum. Electronics* **39**, 1409–1414 (2003).
40. I. De Leon, P. Berini, Amplification of long-range surface plasmons by a dipolar gain medium. *Nat. Photonics* **4**, 382–387 (2010).
41. C. E. Rüter, K. G. Makris, R. El-Ganainy, D. N. Christodoulides, M. Segev, D. Kip, Observation of parity–time symmetry in optics. *Nat. Phys.* **6**, 192–195 (2010).
42. C. M. Bender, S. Boettcher, Real spectra in non-Hermitian Hamiltonians having PT symmetry. *Phys. Rev. Lett.* **80**, 5243 (1998).
43. N. Matsumoto, T. Hosokura, K. Kageyama, H. Takagi, Y. Sakabe, M. Hangyo, Analysis of dielectric response of $TiO_2$ in terahertz frequency region by general harmonic oscillator model. *Jp. J. Appl. Phys.* **47**, 7725 (2008).
44. K. Berdel, J. G. Rivas, P. H. Bolivar, P. J. I. De Maagt, H. Kurz, Temperature dependence of the permittivity and loss tangent of high-permittivity materials at terahertz frequencies. *IEEE T. Microw. Theory* **53**, 1266–1271 (2005).
45. S. C. Howells, L. A. Schlie, Transient terahertz reflection spectroscopy of undoped InSb from 0.1 to 1.1 THz. *Appl. Phys. Lett.* **69**, 550–552 (1996).
46. T. H. Isaac, J. G. Rivas, J. R. Sambles, W. L. Barnes, E. Hendry, Surface plasmon mediated transmission of subwavelength slits at THz frequencies. *Phys. Rev. B* **77**, 113411 (2008).



**Acknowledgments:** We thank S. Torquato for his encouragement on our research on disordered systems, and we thank the anonymous reviewers for their valuable comments and insights. **Funding:** This work was supported by the National Research Foundation of Korea (NRF) through the Global Frontier Program NRF-2014M3A6B3063708 and the Global Research Laboratory Program K20815000003, which are all funded by the Ministry of Science, ICT and Future Planning of the Korean government. S.Y. was supported by the Basic Science Research Program (2016R1A6A3A04009723) through the NRF, funded by the Ministry of Education of the Korean government. **Author contributions:** S.Y. conceived the presented idea, developed the theory, and performed the computations. X.P. contributed to the analysis of wave transport. X.P. and J.H. verified the analytical methods. N.P. encouraged S.Y. to investigate the inverse design and small-world nature of eigensystems while supervising the findings of this work. All authors discussed the results and contributed to the final manuscript. **Competing interests:** The authors declare that they have no competing interests. **Data and materials availability:** All data needed to evaluate the conclusions in the paper are present in the paper and/or the Supplementary Materials. Additional data related to this paper may be requested from the authors.

Submitted 18 December 2015
Accepted 8 September 2016
Published 14 October 2016
10.1126/sciadv.1501851

**Citation:** S. Yu, X. Piao, J. Hong, N. Park, Metadisorder for designer light in random systems. *Sci. Adv.* **2**, e1501851 (2016).